

A Nonnested Augmented Subspace Method for Eigenvalue Problems with Curved Interfaces*

Haikun Dang[†], Hehu Xie[‡], Gang Zhao[§] and Chenguang Zhou[¶]

Abstract

In this paper, we present a nonnested augmented subspace algorithm and its multilevel correction method for solving eigenvalue problems with curved interfaces. The augmented subspace algorithm and the corresponding multilevel correction method are designed based on a coarse finite element space which is not the subset of the finer finite element space. The nonnested augmented subspace method can transform the eigenvalue problem solving on the finest mesh to the solving linear equation on the same mesh and small scale eigenvalue problem on the low dimensional augmented subspace. The corresponding theoretical analysis and numerical experiments are provided to demonstrate the efficiency of the proposed algorithms.

Keywords. Nonnested augmented subspace method, multilevel correction method, finite element method, eigenvalue problem, curved interface.

AMS subject classifications. 65N30, 65N25, 65L15, 65B99.

1 Introduction

There exist a lot of eigenvalue problems in scientific research and practical engineering. Especially, along with the development of modern science and technology, the scale of eigenvalue problems is becoming larger and larger, which leads to the urgent demand for efficient numerical methods for eigenvalue problems. It is well known that multigrid methods have been developed to be very mature and produced an almost complete set of solvers and theoretical systems for solving linear boundary value problems [7, 8, 9, 10, 11, 23, 45, 46, 47, 60, 61, 62]. On the contrary, the applications of the multigrid methods to solving nonlinear problems and eigenvalue problems are very few and need more attentions. In order to use the multigrid method, the normal way is to linearize the nonlinear problems with some type of nonlinear iteration. Then we solve the linearized equations with the help of multigrid methods. This is always called the outer iteration (nonlinear iteration) plus the inner iteration (multigrid iteration). Although the multigrid method has the

*This work was supported in part by the National Key Research and Development Program of China (2019YFA0709601), Science Challenge Project (No. TZ2016002), National Natural Science Foundations of China (NSFC 11771434, 91730302, 91630201), the National Center for Mathematics and Interdisciplinary Science, CAS.

[†]ICMSEC, LSEC, NCMIS, Academy of Mathematics and Systems Science, Chinese Academy of Sciences, Beijing 100190, China, and School of Mathematical Sciences, University of Chinese Academy of Sciences, Beijing, 100049, China (danghaikun@lsec.cc.ac.cn).

[‡]ICMSEC, LSEC, NCMIS, Academy of Mathematics and Systems Science, Chinese Academy of Sciences, Beijing 100190, China, and School of Mathematical Sciences, University of Chinese Academy of Sciences, Beijing, 100049, China (hxie@lsec.cc.ac.cn).

[§]ICMSEC, LSEC, NCMIS, Academy of Mathematics and Systems Science, Chinese Academy of Sciences, Beijing 100190, China, and School of Mathematical Sciences, University of Chinese Academy of Sciences, Beijing, 100049, China (zhaog6@lsec.cc.ac.cn).

[¶]ICMSEC, LSEC, NCMIS, Academy of Mathematics and Systems Science, Chinese Academy of Sciences, Beijing 100190, China, and School of Mathematical Sciences, University of Chinese Academy of Sciences, Beijing, 100049, China (zhouchenguang@lsec.cc.ac.cn).

best efficiency for the inner iteration, the total computational work is controlled by the number of outer iteration steps. When the concerned problem has strong nonlinearity and needs many outer iteration steps, the computational work will be very large even though the multigrid method is used for the inner iteration. Based on this understanding, the application of multigrid algorithms does not affect the outer iteration and can not make the total computational work be independent of the nonlinear iterations.

A special example among nonlinear equations is the eigenvalue problem which originates from applied mathematics, physics, chemistry, cybernetics and other disciplines. Similarly, the multigrid algorithms for eigenvalue problems have not been developed so well, even there exist some numerical methods from Hackbusch [22], Brandt [11], Shaidurov [46] and so on. Since these multigrid methods are designed based on inverse power method or Rayleigh quotient iteration, we always need to solve almost singular linear equations during the whole process. For this reason, the corresponding computational work depends on eigenvalue distributions. It is more difficult to design some type of numerical methods for solving the eigenvalue problems with the optimal computational complexity and storage as that for the linear boundary value problems. From this point of view, the application of multigrid method does not leads to a new eigensolver.

In recent years, multilevel correction methods and their corresponding multigrid algorithms for eigenvalue problems and nonlinear problems have been proposed and discussed in [14, 15, 20, 21, 24, 25, 26, 27, 29, 30, 31, 36, 37, 38, 39, 42, 48, 50, 49, 51, 52, 53, 54, 55, 56, 57, 58, 63, 65, 64, 66]. This type of multilevel correction methods can transform the eigenvalue problem solving into solving standard linear equations and eigenvalue problems in a very low dimensional space. This process makes the computational work for solving the eigenvalue problems be equivalent to that for solving the corresponding linear problems by adjusting the low-dimensional spaces. Among these existing multilevel correction and multigrid methods, the concerned sequence of meshes are required to be nested which means the finite element space defined on the coarse mesh is a subset of the one defined on the finer meshes. This standard requirement forbids the applications of multilevel correction methods in the adaptive triangulations which are generated by moving meshes [18, 34, 35, 40, 41]. For example, when the eigenvalue problem is defined on the domain with curved interfaces and piecewise constant coefficients, in order to guarantee the approximation accuracy for the curve interface, we can not produce the nested coarse and finer meshes for the multilevel correction method. The aim of this paper is to propose a type of nonnested augmented subspace method and then multilevel correction scheme for solving the eigenvalue problems with curved interfaces and piecewise constant coefficients.

An outline of this paper goes as follows. In Section 2, we introduce the finite element method for the eigenvalue problem and the corresponding error estimate theory. A nonnested augmented subspace method for the eigenvalue problem is proposed in Section 3. In Section 4, we design a type of multilevel correction method for the eigenvalue problem based on the augmented subspace method in Section 3. In Section 5, four numerical examples are provided to validate the theoretical results and illustrate the efficiency of proposed algorithms in this paper. Finally, some concluding remarks are given in the last section.

2 Finite element method of the eigenvalue problem

This section is devoted to introducing some notation and the standard finite element method for the eigenvalue problem. In this paper, we shall use the standard notation for Sobolev spaces $W^{s,p}(\Omega)$ and their associated norms and semi-norms (cf. [1]). For $p = 2$, we denote $H^s(\Omega) = W^{s,2}(\Omega)$ and $H_0^1(\Omega) = \{v \in H^1(\Omega) : v|_{\partial\Omega} = 0\}$, where $v|_{\partial\Omega} = 0$ is in the sense of trace, $\|\cdot\|_{s,\Omega} = \|\cdot\|_{s,2,\Omega}$. In some places, $\|\cdot\|_{s,2,\Omega}$ should be viewed as piecewise defined if it is necessary. The letter C (with or without subscripts) denotes a generic positive constant which may be different at its different occurrences throughout the paper.

In this paper, we are concerned with the following second order elliptic eigenvalue problem: Find (λ, u) such that

$$\begin{cases} -\nabla \cdot (\mathcal{A}\nabla u) = \lambda u, & \text{in } \Omega, \\ [u] = 0, \quad [\mathbf{n}_\Gamma \mathcal{A}\nabla u] = 0, & \text{on } \Gamma, \\ u = 0, & \text{on } \partial\Omega, \end{cases} \quad (2.1)$$

where the computing domain Ω has curved interfaces Γ which denotes the set of all involved interfaces, $\mathcal{A} = (a_{i,j})_{d \times d}$ is a symmetric positive definite matrix and $a_{i,j} \in W^{0,\infty}(\Omega)$ ($i, j = 1, 2, \dots, d$) are piecewise constants. In this paper, $[v] := (v|_{\Omega_i})|_\Gamma - (v|_{\Omega_j})|_\Gamma$ for any function v in $H^1(\Omega)$, where Ω_i and Ω_j are any two adjacent subdomains and \mathbf{n}_Γ denotes a unit normal vector from Ω_i to Ω_j across the interface. Figure 1 shows an example of computing domain with four curved interfaces.

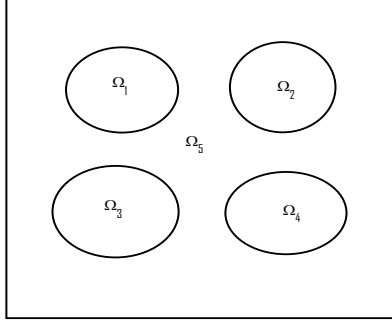


Figure 1: Domain with curved interfaces

In order to use the finite element method to solve the eigenvalue problem (2.1), we define the corresponding variational form as follows: Find $(\lambda, u) \in \mathcal{R} \times V$ such that $a(u, u) = 1$ and

$$a(u, v) = \lambda b(u, v), \quad \forall v \in V, \quad (2.2)$$

where $V := H_0^1(\Omega)$, and the bilinear forms $a(\cdot, \cdot)$ and $b(\cdot, \cdot)$ are defined as

$$a(u, v) = \int_{\Omega} \mathcal{A}\nabla u \cdot \nabla v d\Omega, \quad b(u, v) = \int_{\Omega} uv d\Omega. \quad (2.3)$$

The norms $\|\cdot\|_a$ and $\|\cdot\|_b$ are defined by

$$\|v\|_a = \sqrt{a(v, v)} \quad \text{and} \quad \|v\|_b = \sqrt{b(v, v)}.$$

It is easy to know that $a(u, v)$ satisfies boundedness and coercive property on V , i.e.,

$$a(u, v) \leq C_a \|u\|_{1,\Omega} \|v\|_{1,\Omega} \quad \text{and} \quad c_a \|u\|_{1,\Omega}^2 \leq a(u, u), \quad \forall u, v \in V. \quad (2.4)$$

Then the norm $\|\cdot\|_a$ is equivalent to the one $\|\cdot\|_1$.

It is standard that the eigenvalue problem (2.2) has an eigenvalue sequence $\{\lambda_j\}$ (cf. [3, 13]):

$$0 < \lambda_1 < \lambda_2 \leq \dots \leq \lambda_k \leq \dots, \quad \lim_{k \rightarrow \infty} \lambda_k = \infty,$$

and the associated eigenfunctions

$$u_1, u_2, \dots, u_k, \dots,$$

where $a(u_i, u_j) = \delta_{ij}$ (δ_{ij} is the Kronecker function). In the sequence $\{\lambda_j\}$, the λ_j are repeated based on their geometric multiplicity.

For the theoretical analysis in this paper, we present the definition corresponding to the smallest eigenvalue λ_1 (c.f. [3, 13]) as follows

$$\lambda_1 = \min_{0 \neq w \in V} \frac{a(w, w)}{b(w, w)}. \quad (2.5)$$

Now, we come to introduce the finite element method for (2.2). First, let us define the finite element space. Let \mathcal{T}_h be a regular partition of $\Omega \subset \mathbb{R}^d$ ($d = 2, 3$) which means a two-dimensional domain is divided into regular triangles or quadrangles (a three-dimensional domain is divided into tetrahedrons or hexahedrons) [12, 17]. Denote the diameter of a element $K \in \mathcal{T}_h$ by h_K , and h describes the maximum diameter of all elements of \mathcal{T}_h . In order to guarantee the accuracy of finite element spaces, the domain is usually partitioned along the interior edges (or faces) so that the partition has a certain approximating accuracy to the curved interfaces. Based on the mesh \mathcal{T}_h , we can construct a finite element space denoted by $V_h \subset V$. For simplicity, we set V_h as the linear finite element space which is defined as follows

$$V_h = \{v_h \in C(\Omega) \mid v_h|_K \in \mathcal{P}_1, \quad \forall K \in \mathcal{T}_h\} \cap H_0^1(\Omega), \quad (2.6)$$

where \mathcal{P}_1 denotes the linear function space. Since the appearance of curved interfaces and the accuracy requirement, there is no nested sequence of meshes as that for the polygonal domains. Then we have no nested sequence of finite element spaces which is always needed in the multigrid method.

Based on the space V_h , the standard finite element scheme for eigenvalue problem (2.2) is: Find $(\bar{\lambda}_h, \bar{u}_h) \in \mathcal{R} \times V_h$ such that $a(\bar{u}_h, \bar{u}_h) = 1$ and

$$a(\bar{u}_h, v_h) = \bar{\lambda}_h b(\bar{u}_h, v_h), \quad \forall v_h \in V_h. \quad (2.7)$$

From [3, 13], we know that the discrete eigenvalue problem (2.7) has an eigenvalue sequence

$$0 < \bar{\lambda}_{1,h} \leq \bar{\lambda}_{2,h} \leq \cdots \leq \bar{\lambda}_{k,h} \leq \cdots \leq \bar{\lambda}_{N_h,h},$$

and the corresponding discrete eigenfunction sequence

$$\bar{u}_{1,h}, \bar{u}_{2,h}, \cdots, \bar{u}_{k,h}, \cdots, \bar{u}_{N_h,h},$$

where $a(\bar{u}_{i,h}, \bar{u}_{j,h}) = \delta_{ij}$, $1 \leq i, j \leq N_h$ ($N_h = \dim V_h$).

In order to measure the error of the finite element space to the desired function, we define the following notation

$$\delta(w, V_h) = \inf_{v_h \in V_h} \|w - v_h\|_a, \quad \text{for } w \in V. \quad (2.8)$$

In this paper, we also need the following quantity for error analysis:

$$\eta_a(V_h) = \sup_{\substack{f \in L^2(\Omega) \\ \|f\|_b=1}} \inf_{v_h \in V_h} \|Tf - v_h\|_a, \quad (2.9)$$

where $T : L^2(\Omega) \rightarrow V$ is defined as

$$a(Tf, v) = b(f, v), \quad \forall v \in V \quad \text{for } f \in L^2(\Omega). \quad (2.10)$$

It is known that $\eta_a(V_h) \rightarrow 0$ when $h \rightarrow 0$ (c.f. [2, 16, 33]). Based on the finite element space V_h , we define the finite element projection operator $\mathcal{P}_h : V \rightarrow V_h$ as follows

$$a(w, v_h) = a(\mathcal{P}_h w, v_h), \quad \forall v_h \in V_h, \quad \text{for } w \in V. \quad (2.11)$$

It is obvious that $\delta(u, V_h) = \|u - \mathcal{P}_h u\|_a$.

In order to introduce and analyze the nonnested augmented subspace algorithm and the corresponding multilevel correction method for the eigenvalue problem, we state the following error estimate results from [56] which include only explicit constants. For more details, please refer to [56].

It should be pointed out that the following error estimate results hold for general finite-dimensional approximations of eigenvalue problems.

Lemma 2.1. ([56]) *Let (λ, u) be an exact eigenpair of the eigenvalue problem (2.2). Assume the eigenpair approximation $(\bar{\lambda}_{i,h}, \bar{u}_{i,h})$ has the property that $\bar{\mu}_{i,h} = 1/\bar{\lambda}_{i,h}$ is the closest to $\mu = 1/\lambda$. The corresponding spectral projection operators $E_{i,h} : V \mapsto \text{span}\{\bar{u}_{i,h}\}$ and $E : V \mapsto \text{span}\{u\}$ are defined as follows*

$$\begin{aligned} a(E_{i,h} w, \bar{u}_{i,h}) &= a(w, \bar{u}_{i,h}), & \text{for } w \in V, \\ a(E w, u) &= a(w, u), & \text{for } w \in V. \end{aligned}$$

The finite element approximation $\bar{u}_{i,h}$ has the following error estimate

$$\|u - E_{i,h} u\|_a \leq \sqrt{1 + \frac{\bar{\mu}_{1,h}}{\delta_{\lambda,h}^2} \eta_a^2(V_h)} \delta(u, V_h), \quad (2.12)$$

where $\eta_a(V_h)$ is defined from (2.9) and $\delta_{\lambda,h}$ is defined as

$$\delta_{\lambda,h} := \min_{j \neq i} |\bar{\mu}_{j,h} - \mu| = \min_{j \neq i} \left| \frac{1}{\bar{\lambda}_{j,h}} - \frac{1}{\lambda} \right|. \quad (2.13)$$

Moreover, the eigenfunction approximation $\bar{u}_{i,h}$ has the following error estimate corresponding to L^2 -norm

$$\|u - E_{i,h} u\|_b \leq \left(1 + \frac{\bar{\mu}_{1,h}}{\delta_{\lambda,h}}\right) \eta_a(V_h) \|u - E_{i,h} u\|_a. \quad (2.14)$$

For the convenience of analysis, we state the following corollary which is based on Lemma 2.1.

Corollary 2.1. *Under the assumption of Lemma 2.1, we have following error estimates*

$$\|\lambda u - \bar{\lambda}_{i,h} \bar{u}_{i,h}\|_b \leq C_\lambda \eta_a(V_h) \|u - \bar{u}_{i,h}\|_a, \quad (2.15)$$

$$\|u - \bar{u}_{i,h}\|_a \leq \frac{1}{1 - D_\lambda \eta_a(V_h)} \delta(u, V_h), \quad (2.16)$$

where the constants C_λ and D_λ are defined as

$$C_\lambda = 2|\lambda| \left(1 + \frac{1}{\lambda_1 \delta_{\lambda,h}}\right) + \bar{\lambda}_{i,h} \sqrt{1 + \frac{1}{\lambda_1 \delta_{\lambda,h}^2} \eta_a^2(V_h)}, \quad (2.17)$$

$$D_\lambda = \frac{1}{\sqrt{\lambda_1}} \left(2|\lambda| \left(1 + \frac{1}{\lambda_1 \delta_{\lambda,h}}\right) + \bar{\lambda}_{i,h} \sqrt{1 + \frac{1}{\lambda_1 \delta_{\lambda,h}^2} \eta_a^2(V_h)}\right). \quad (2.18)$$

3 Augmented subspace algorithm

In this section, a nonnested augmented subspace method will be designed for eigenvalue problems. With the help of the coarse space on a coarse mesh, the proposed method can transform the solution of the eigenvalue problem to the corresponding linear boundary value problems and eigenvalue

problems on a very low dimensional augmented space. Different from the augmented subspace or multilevel correction scheme from [38, 49, 50, 56], the coarse space here is not the subspace of the finer finite element spaces.

In order to define the nonnested augmented subspace method, we generate a coarse mesh \mathcal{T}_H with the mesh size H and the coarse linear finite element space V_H is defined on the mesh \mathcal{T}_H . The grids \mathcal{T}_H and \mathcal{T}_h have no nested properties, which results in $V_H \not\subset V_h$. With the help of V_H , an augmented subspace can be designed as $V_{H,h} := V_H + \text{span}\{\tilde{u}_h\}$, where $\tilde{u}_h \in V_h$ denotes a finite element function defined on the finer mesh. Although V_H and V_h have no nested properties, the augmented subspace $V_{H,h}$ is a finite-dimensional subspace of V . Therefore, we know that the error estimates in Lemma 2.1 and Corollary 2.1 still hold for $V_{H,h}$.

Assume we have obtained an approximation $(\lambda_h^{(\ell)}, u_h^{(\ell)})$ for a certain exact eigenpair. The augmented subspace iteration algorithm defined by Algorithm 1 is used to improve the accuracy of $(\lambda_h^{(\ell)}, u_h^{(\ell)})$. Here the superscript ℓ denotes iteration index and $(\lambda_h^{(\ell)}, u_h^{(\ell)})$ is the inputted eigenpair.

Algorithm 1: Augmented subspace iteration algorithm

1. Define the following linear boundary value problem: Find $\hat{u}_h^{(\ell+1)} \in V_h$ such that

$$a(\hat{u}_h^{(\ell+1)}, v_h) = \lambda_h^{(\ell)} b(u_h^{(\ell)}, v_h), \quad \forall v_h \in V_h. \quad (3.1)$$

Solve (3.1) with initial value $u_{h_k}^{(\ell)}$ and some algebraic multigrid steps to obtain a new eigenfunction approximation $\tilde{u}_h^{(\ell+1)}$ which satisfies the following estimate

$$\|\hat{u}_h^{(\ell+1)} - \tilde{u}_h^{(\ell+1)}\|_a \leq \theta \|\hat{u}_h^{(\ell+1)} - u_{h_k}^{(\ell)}\|_a, \quad (3.2)$$

where $\theta < 1$ is independent of the mesh size h and the iteration number ℓ .

2. Define the augmented subspace $V_{H,h} = V_H + \text{span}\{\tilde{u}_h^{(\ell+1)}\}$ and solve the following eigenvalue problem: Find $(\lambda_h^{(\ell+1)}, u_h^{(\ell+1)}) \in \mathbb{R} \times V_{H,h}$ such that $a(u_h^{(\ell+1)}, u_h^{(\ell+1)}) = 1$ and

$$a(u_h^{(\ell+1)}, v_{H,h}) = \lambda_h^{(\ell+1)} b(u_h^{(\ell+1)}, v_{H,h}), \quad \forall v_{H,h} \in V_{H,h}. \quad (3.3)$$

Solve (3.3) and the output $(\lambda_h^{(\ell+1)}, u_h^{(\ell+1)})$ is chosen such that $u_h^{(\ell+1)}$ has the largest component in $\text{span}\{\tilde{u}_h^{(\ell+1)}\}$ among all eigenfunctions of (3.3).

Summarize abovementioned two steps by defining

$$(\lambda_h^{(\ell+1)}, u_h^{(\ell+1)}) = \text{AugSubspace}(\lambda_h^{(\ell)}, u_h^{(\ell)}, V_H, V_h).$$

In order to simplify the notation, we assume the eigenvalue gap $\delta_{\lambda,h}$ has a uniform lower bound which is denoted by δ_λ (which can be seen as the “true” separation of the eigenvalue λ from others). This assumption is reasonable when the mesh size is small enough. We refer to [44, Theorem 4.6] and Lemma 2.1 in this paper for details of the dependence of error estimates on the eigenvalue gap.

Theorem 3.1. *Assume there exists an exact eigenpair (λ, u) such that the eigenpair approximation $(\lambda_{h_k}^{(\ell)}, u_{h_k}^{(\ell)})$ satisfies*

$$\|\lambda u - \lambda_{h_k}^{(\ell)} u_{h_k}^{(\ell)}\|_b \leq \bar{C}_\lambda \eta_\alpha(V_H) \|u - u_{h_k}^{(\ell)}\|_a. \quad (3.4)$$

Then the eigenpair approximation $(\lambda_h^{(\ell+1)}, u_h^{(\ell+1)}) \in \mathbb{R} \times V_h$ obtained by Algorithm 1 satisfies

$$\|u - u_h^{(\ell+1)}\|_a \leq \gamma \|u - u_h^{(\ell)}\|_a + \zeta \|u - \mathcal{P}_h u\|_a, \quad (3.5)$$

$$\|\lambda u - \lambda_h^{(\ell+1)} u_h^{(\ell+1)}\|_b \leq \bar{C}_\lambda \eta_a(V_H) \|u - u_h^{(\ell+1)}\|_a, \quad (3.6)$$

where the constants γ , ζ , \bar{C}_λ and \bar{D}_λ are defined as

$$\gamma = \frac{1}{1 - \bar{D}_\lambda \eta_a(V_H)} \left(\theta + (1 + \theta) \frac{\bar{C}_\lambda}{\sqrt{\lambda_1}} \eta_a(V_H) \right), \quad (3.7)$$

$$\zeta = \frac{1 + \theta}{1 - \bar{D}_\lambda \eta_a(V_H)}, \quad (3.8)$$

$$\bar{C}_\lambda = 2|\lambda| \left(1 + \frac{1}{\lambda_1 \delta_\lambda} \right) + \bar{\lambda}_{i,H} \sqrt{1 + \frac{1}{\lambda_1 \delta_\lambda^2} \eta_a^2(V_H)}, \quad (3.9)$$

$$\bar{D}_\lambda = \frac{1}{\sqrt{\lambda_1}} \left(2|\lambda| \left(1 + \frac{1}{\lambda_1 \delta_\lambda} \right) + \bar{\lambda}_{i,H} \sqrt{1 + \frac{1}{\lambda_1 \delta_\lambda^2} \eta_a^2(V_H)} \right). \quad (3.10)$$

Proof. From (2.5), (2.2), (2.11), (3.1) and (3.4), the following estimate holds for any $w \in V_h$,

$$\begin{aligned} a(\mathcal{P}_h u - \hat{u}_h^{(\ell+1)}, w) &= b((\lambda u - \lambda_h^{(\ell)} u_h^{(\ell)}), w) \leq \|\lambda u - \lambda_h^{(\ell)} u_h^{(\ell)}\|_b \|w\|_b \\ &\leq \bar{C}_\lambda \eta_a(V_H) \|u - u_h^{(\ell)}\|_a \|w\|_b \leq \frac{1}{\sqrt{\lambda_1}} \bar{C}_\lambda \eta_a(V_H) \|u - u_h^{(\ell)}\|_a \|w\|_a. \end{aligned} \quad (3.11)$$

Taking $w = \mathcal{P}_h u - \hat{u}_h^{(\ell+1)}$ in (3.11) implies the following estimate

$$\|\mathcal{P}_h u - \hat{u}_h^{(\ell+1)}\|_a \leq \frac{\bar{C}_\lambda}{\sqrt{\lambda_1}} \eta_a(V_H) \|u - u_h^{(\ell)}\|_a. \quad (3.12)$$

Combining (3.2) with (3.12), it follows that

$$\begin{aligned} \|\mathcal{P}_h u - \tilde{u}_h^{(\ell+1)}\|_a &\leq \|\mathcal{P}_h u - \hat{u}_h^{(\ell+1)}\|_a + \|\tilde{u}_h^{(\ell+1)} - \hat{u}_h^{(\ell+1)}\|_a \\ &\leq \|\mathcal{P}_h u - \hat{u}_h^{(\ell+1)}\|_a + \theta \|\hat{u}_h^{(\ell+1)} - u_h^{(\ell)}\|_a \\ &\leq \|\mathcal{P}_h u - \hat{u}_h^{(\ell+1)}\|_a + \theta \|\hat{u}_h^{(\ell+1)} - \mathcal{P}_h u\|_a + \theta \|\mathcal{P}_h u - u_h^{(\ell)}\|_a \\ &\leq (1 + \theta) \|\mathcal{P}_h u - \hat{u}_h^{(\ell+1)}\|_a + \theta \|\mathcal{P}_h u - u\|_a + \theta \|u - u_h^{(\ell)}\|_a \\ &\leq \left(\theta + (1 + \theta) \frac{\bar{C}_\lambda}{\sqrt{\lambda_1}} \eta_a(V_H) \right) \|u - u_h^{(\ell)}\|_a + \theta \|u - \mathcal{P}_h u\|_a. \end{aligned} \quad (3.13)$$

Similarly, the discrete eigenvalue problem (3.3) can be regarded as a subspace approximation to the eigenvalue problem (2.2). Thus, from (2.16), (3.13), Lemma 2.1 and Corollary 2.1, there hold following error estimates

$$\begin{aligned} \|u - u_h^{(\ell+1)}\|_a &\leq \frac{1}{1 - \bar{D}_\lambda \eta_a(V_{H,h})} \inf_{v_{H,h_k} \in V_{H,h}} \|u - v_{H,h_k}\|_a \\ &\leq \frac{1}{1 - \bar{D}_\lambda \eta_a(V_H)} \|u - \tilde{u}_h^{(\ell+1)}\|_a \\ &\leq \frac{1}{1 - \bar{D}_\lambda \eta_a(V_H)} (\|u - \mathcal{P}_h u\|_a + \|\mathcal{P}_h u - \tilde{u}_h^{(\ell+1)}\|_a) \\ &\leq \gamma \|u - u_h^{(\ell)}\|_a + \zeta \|u - \mathcal{P}_h u\|_a, \end{aligned}$$

and

$$\|\lambda u - \lambda_h^{(\ell+1)} u_h^{(\ell+1)}\|_b \leq \bar{C}_\lambda \eta(V_{H,h_k}) \|u - u_h^{(\ell+1)}\|_a \leq \bar{C}_\lambda \eta(V_H) \|u_h - u_h^{(\ell+1)}\|_a.$$

Thus the desired results (3.5) and (3.6) are obtained and the proof is complete. \square

Eventhough there is no nested sequence of meshes, some efficient numerical algorithms such as algebraic multigrid (AMG) method can be adopted as the linear solver for (3.1).

Corollary 3.1. *Under the conditions of Theorem 3.1, after executing L augmented subspace iteration step defined by Algorithm 1, the resultant eigenpair approximation $(\lambda_h^{(L)}, u_h^{(L)}) \in \mathbb{R} \times V_h$ has following error estimates*

$$\|u - u_h^{(L)}\|_a \leq \gamma^L \|u - u_h^{(0)}\|_a + \frac{1 - \gamma^L}{1 - \gamma} \zeta \|u - \mathcal{P}_h u\|_a, \quad (3.14)$$

$$\|\lambda u - \lambda_h^{(L)} u_h^{(L)}\|_b \leq \bar{C} \lambda \eta_a(V_H) \|u - u_h^{(L)}\|_a. \quad (3.15)$$

Proof. According to (3.5) and recursive argument, it follows that

$$\begin{aligned} \|u - u_h^{(L)}\|_a &\leq \gamma \|u - u_h^{(L-1)}\|_a + \zeta \|u - \mathcal{P}_h u\|_a \\ &\leq \gamma (\gamma \|u - u_h^{(L-2)}\|_a + \zeta \|u - \mathcal{P}_h u\|_a) + \zeta \|u - \mathcal{P}_h u\|_a \\ &\leq \gamma^L \|u - u_h^{(0)}\|_a + \sum_{\ell=0}^{L-1} \gamma^\ell \zeta \|u - \mathcal{P}_h u\|_a \\ &= \gamma^L \|u - u_h^{(0)}\|_a + \frac{1 - \gamma^L}{1 - \gamma} \zeta \|u - \mathcal{P}_h u\|_a, \end{aligned}$$

which proves the inequality (3.14). Similarly to the proof of Theorem 3.1, the desired result (3.15) can also be deduced. \square

From the convergence results of Theorem 3.1 and the definition (3.7), it is easy to know that γ is less than 1 and independent of the finer mesh size h when H is sufficiently small.

Remark 3.1. *The eigenpair solution $(\lambda_h^{(\ell+1)}, u_h^{(\ell+1)})$ of (3.3) is an algebraic approximation to the following eigenvalue problem: Find $(\bar{\lambda}_{H,h}, \bar{u}_{H,h}) \in \mathcal{R} \times (V_H + V_h \setminus V_H)$ such that $a(\bar{u}_{H,h}, \bar{u}_{H,h}) = 1$ and*

$$a(\bar{u}_{H,h}, v_{H,h}) = \bar{\lambda}_{H,h} b(\bar{u}_{H,h}, v_{H,h}), \quad \forall v_{H,h} \in V_{H,h}, \quad (3.16)$$

where $V_h \setminus V_H$ denotes the space which are produced by deleting the components in V_H from V_h .

In Algorithm 1, the space $V_{H,h}$ is defined based on V_H on the coarse mesh and V_h on the finer mesh. Since $V_H \not\subset V_h$, the augmented subspace method defined by Algorithm 1 can be combined with the moving mesh method where the sequence of meshes does not have nested property [18, 34, 35, 40, 41]. This is the most important contribution of this paper. Because of $V_H \not\subset V_h$, the definition of the interpolation operator $I_H^h : V_H \rightarrow V_h$ is different from the standard one which is defined on the nested meshes \mathcal{T}_H and \mathcal{T}_h . For the detailed construction and implementation, please refer to the documentation of finite element package FreeFem++ [28, 32].

Now, we consider the details for solving the small scale eigenvalue problem (3.3). Let N_H and $\{\psi_{j,H}\}_{1 \leq j \leq N_H}$ denote the dimension and Lagrange basis functions for the coarse finite element space V_H . The function in $V_{H,h}$ can be denoted by $u_{H,h} = u_H + \xi \tilde{u}_h$. Solving eigenvalue problem (3.3) is to obtain the function $u_H \in V_H$ and the value $\xi \in \mathcal{R}$. Let $u_H = \sum_{j=1}^{N_H} u_j \psi_{j,H}$ and define the vector $\mathbf{u}_H = [u_1, \dots, u_{N_H}]^T$. The corresponding matrix version of (3.3) can be defined as follows

$$\begin{pmatrix} A_H & a_h \\ a_h^T & \alpha \end{pmatrix} \begin{pmatrix} \mathbf{u}_H \\ \xi \end{pmatrix} = \lambda_h \begin{pmatrix} B_H & b_h \\ b_h^T & \beta \end{pmatrix} \begin{pmatrix} \mathbf{u}_H \\ \xi \end{pmatrix}, \quad (3.17)$$

where $\mathbf{u}_H \in \mathcal{R}^{N_H \times 1}$ and $\xi \in \mathcal{R}$.

For understanding the proposed method, we introduce the assembling method for the matrices A_H and B_H , vectors a_h and b_h , scalars α and β .

The matrix A_H is defined as

$$(A_H)_{i,j} = (\mathcal{A}\nabla\psi_{i,H}, \nabla\psi_{j,H}) = \int_{\Omega} \nabla\psi_{i,H} \cdot \mathcal{A}\nabla\psi_{j,H} d\Omega, \quad 1 \leq i, j \leq N_H. \quad (3.18)$$

In order to obtain the same precision as V_h , we need to calculate the integral in (3.18) on the finer mesh \mathcal{T}_h . This is because we need to guarantee the accuracy for approximating the curved interfaces to reach the same level as \mathcal{T}_h . Therefore, we use the following way

$$(A_H)_{i,j} = \sum_{K \in \mathcal{T}_h} \int_K \nabla\psi_{i,H} \cdot \mathcal{A}\nabla\psi_{j,H} dK, \quad 1 \leq i, j \leq N_H. \quad (3.19)$$

Similarly, the assembling method for the mass matrix B_H can be given as follows

$$(B_H)_{i,j} = \sum_{K \in \mathcal{T}_h} \int_K \psi_{i,H} \psi_{j,H} dK, \quad 1 \leq i, j \leq N_H. \quad (3.20)$$

Now we concentrate on assembling the vector a_h , which is defined as follows

$$(a_h)_i = \int_{\Omega} \nabla\psi_{i,H} \cdot \mathcal{A}\nabla\tilde{u}_h d\Omega, \quad 1 \leq i \leq N_H. \quad (3.21)$$

Since the finite element function \tilde{u}_h is defined on the finer mesh \mathcal{T}_h , the assembling of a_h needs to be implemented on \mathcal{T}_h , i.e.,

$$(a_h)_i = \sum_{K \in \mathcal{T}_h} \int_K \nabla\psi_{i,H} \cdot \mathcal{A}\nabla\tilde{u}_h dK, \quad 1 \leq i \leq N_H. \quad (3.22)$$

Similarly, the vector b_h should be assembled in the following way

$$(b_h)_i = \sum_{K \in \mathcal{T}_h} \int_K \psi_{i,H} \tilde{u}_h dK, \quad 1 \leq i \leq N_H. \quad (3.23)$$

Based on the structure of $V_{H,h}$, the scalars α and β are assembled as follows

$$\alpha = \int_{\Omega} \nabla\tilde{u}_h \cdot \mathcal{A}\nabla\tilde{u}_h d\Omega = \sum_{K \in \mathcal{T}_h} \int_K \nabla\tilde{u}_h \cdot \mathcal{A}\nabla\tilde{u}_h dK, \quad (3.24)$$

$$\beta = \int_{\Omega} |\tilde{u}_h|^2 d\Omega = \sum_{K \in \mathcal{T}_h} \int_K |\tilde{u}_h|^2 dK. \quad (3.25)$$

After assembling the matrices A_H and B_H , vectors a_h and b_h , scalars α and β , some algebraic eigensolver are adopted to solve the eigenvalue problem (3.17) to obtain \mathbf{u}_H and ξ . For the next iteration, the function $u_H + \xi\tilde{u}_h^{(\ell+1)}$ should be interpolated into the finite element space V_h . With the help of the interpolator operator I_H^h , we can obtain $u_h^{(\ell+1)}$ by the following way

$$u_h^{(\ell+1)} = I_H^h u_H + \xi\tilde{u}_h^{(\ell+1)}. \quad (3.26)$$

According to the definition of Algorithm 1 and the detailed implementing process, it is easy to state the estimate of computational work for the nonnested augmented subspace method. For this aim, we denote the degree of freedom of the finite element space V_h as N_h .

Theorem 3.2. *Assume solving the linear eigenvalue problem (3.17) needs work $\mathcal{O}(M_H)$ ($M_H > N_H$), and the work for solving (3.1) is $\mathcal{O}(N_h)$. Then the computational work included in Algorithm 1 is*

$$\text{Work} = \mathcal{O}(N_h + M_H). \quad (3.27)$$

4 Multilevel correction method

Similarly to the full multigrid method for the linear boundary value problems, we can use the nonnested augmented subspace method defined by Algorithm 1 to build a type of multilevel correction method for the eigenvalue problem (2.2). Different from the existed multilevel correction method in [36, 38, 49, 50], the sequence of meshes has no nested property since the existence of the curved interfaces. The idea to build the multilevel correction method is to use the eigenpair approximations on the coarse mesh as the initial values on the finer mesh for augmented subspace algorithm. The reason to call the proposed method as the multilevel correction method is the sequence of concerned finite element spaces has no nested property.

In order to design the multilevel correction method, we first introduce the sequence of finite element spaces. We generate a coarse mesh \mathcal{T}_H with the mesh size H and the coarse linear finite element space V_H is defined on the mesh \mathcal{T}_H . Then a sequence of meshes \mathcal{T}_{h_k} is generated by some type of mesh tool and the mesh sizes h_k satisfy the following properties

$$h_1 < H, \quad h_k = \frac{1}{\beta} h_{k-1}, \quad k = 2, \dots, n. \quad (4.1)$$

Based on the sequence of meshes \mathcal{T}_{h_k} , we can construct the corresponding linear finite element spaces V_{h_k} ($k = 1, \dots, n$). Although the sequence of spaces V_{h_k} does not have nested properties, the following relationships and error estimates hold

$$\eta_a(V_{h_k}) \approx \frac{1}{\beta} \eta_a(V_{h_{k-1}}), \quad \delta(u, V_{h_{k-1}}) \approx \frac{1}{\beta} \delta(u, V_{h_k}), \quad k = 2, \dots, n. \quad (4.2)$$

The corresponding multilevel correction method is defined by Algorithm 2.

Algorithm 2: Multilevel correction method

1. Solve the eigenvalue problem on V_{h_1} : Find $(\lambda_{h_1}, u_{h_1}) \in \mathbb{R} \times V_{h_1}$ such that

$$a(u_{h_1}, v_{h_1}) = \lambda_{h_1}(u_{h_1}, v_{h_1}), \quad \forall v_{h_1} \in V_{h_1}.$$

2. For $k = 2, \dots, n$, do the following iteration:

- (a) Let $u_{h_k}^{(0)} = u_{h_{k-1}}$ and $\lambda_{h_k}^{(0)} = \lambda_{h_{k-1}}$.

- (b) For $\ell = 0, \dots, L-1$, do the following augmented subspace iteration steps

$$(\lambda_{h_k}^{(\ell+1)}, u_{h_k}^{(\ell+1)}) = \text{AugSubspace}(V_H, \lambda_{h_k}^{(\ell)}, u_{h_k}^{(\ell)}, V_{h_k}).$$

- (c) Define $u_{h_k} = u_{h_k}^{(L)}$ and $\lambda_{h_k} = \lambda_{h_k}^{(L)}$.
-

Based on Theorem 3.1, Corollary 3.1 and the property (4.2), we can deduce the error estimates for Algorithm 2 with some recursive argument.

Theorem 4.1. *Under the condition of (4.2), the eigenpair approximation $(\lambda_{h_n}, u_{h_n}) \in \mathbb{R} \times V_{h_n}$ obtained by Algorithm 2 has the following error estimate*

$$\|u - u_{h_n}\|_a \leq \frac{1 - (\beta\gamma^L)^n}{1 - \beta\gamma^L} \mu \delta(u, V_{h_n}), \quad (4.3)$$

where

$$\mu := \frac{1 - \gamma^L}{1 - \gamma} \zeta. \quad (4.4)$$

Proof. From Lemma 2.1 and the property $\eta_a(V_{h_1}) \leq \eta_a(V_H)$, the eigenfunction approximation u_{h_1} obtained by Step 1 of Algorithm 2 satisfies the following error estimate

$$\|u - u_{h_1}\|_a \leq \frac{1}{1 - \bar{D}_\lambda \eta_a(V_{h_1})} \delta(u, V_{h_1}) \leq \mu \|u - \mathcal{P}_{h_1} u\|_a. \quad (4.5)$$

Combining Corollary 3.1, (4.5) and recursive argument leads to the following estimates

$$\begin{aligned} \|u - u_{h_n}\|_a &\leq \gamma^L \|u - u_{h_{n-1}}\|_a + \mu \|u - \mathcal{P}_{h_n} u\|_a \\ &\leq \gamma^L (\gamma^L \|u - u_{h_{n-2}}\|_a + \mu \|u - \mathcal{P}_{h_{n-1}} u\|_a) + \mu \|u - \mathcal{P}_{h_n} u\|_a \\ &\leq \gamma^{(n-1)L} \|u - u_{h_1}\|_a + \sum_{k=2}^n \gamma^{(n-k)L} \mu \|u - \mathcal{P}_{h_k} u\|_a \\ &\leq \gamma^{(n-1)L} \mu \|u - \mathcal{P}_{h_1} u\|_a + \sum_{k=2}^n \gamma^{(n-k)L} \mu \|u - \mathcal{P}_{h_k} u\|_a \\ &= \sum_{k=1}^n \gamma^{(n-k)L} \mu \delta(u, V_{h_k}) \leq \left(\sum_{k=1}^n \gamma^{(n-k)L} \beta^{n-k} \right) \mu \delta(u, V_{h_n}) \\ &= \left(\sum_{k=1}^n (\beta \gamma^L)^{n-k} \right) \mu \delta(u, V_{h_n}) \leq \frac{1 - (\beta \gamma^L)^n}{1 - \beta \gamma^L} \mu \delta(u, V_{h_n}). \end{aligned}$$

This is the desired result (4.3) and we complete the proof. \square

Now we turn our attention to the estimate of computational work for Algorithm 2. First, we define the dimension of each level of finite element space as $N_{h_k} := \dim V_{h_k}$. Then the following property holds

$$N_{h_k} \approx \left(\frac{1}{\beta} \right)^{d(n-k)} N_{h_n}, \quad k = 1, 2, \dots, n. \quad (4.6)$$

Theorem 4.2. *Assume the conditions of Theorem 3.2 hold and solving the eigenvalue problem in V_{h_1} needs work $\mathcal{O}(M_{h_1})$. Then the computational work involved in Algorithm 2 is*

$$\text{Total Work} = \mathcal{O}(LN_{h_n} + M_{h_1} + LM_H \ln N_{h_n}). \quad (4.7)$$

Proof. From Theorem 3.2 and (4.6), it follows that

$$\begin{aligned} \text{Total Work} &= \mathcal{O} \left(M_{h_1} + \sum_{k=2}^n (L(N_{h_k} + M_H)) \right) \\ &= \mathcal{O} \left(M_{h_1} + L \sum_{k=2}^n \left(\left(\frac{1}{\beta} \right)^{n-k} N_{h_n} + M_H \right) \right) \\ &= \mathcal{O}(LN_{h_n} + M_{h_1} + LM_H \ln N_{h_n}). \end{aligned}$$

Thus the proof is complete. \square

Based on the definition and the corresponding convergence theory, we can find an interesting property that Algorithm 1 can work for only one single eigenpair. During the multilevel correction process, there is no orthogonalization in the high dimension space V_{h_k} with $k \geq 2$. Because of avoiding doing the time-consuming orthogonalization in the high dimensional spaces, the augmented subspace iteration algorithm improves the scalability for solving the eigenvalue problem. Compared with the traditional eigensolvers based on the Krylov subspaces, the coarse space V_H

from the augmented subspace $V_{H,h}$ has the approximation property to general functions (check the definition of $\eta_a(V_H)$ in (2.9)). This is obviously different from the property of the Krylov subspaces which can only approximate the specific functions [44]. This is the reason why Algorithm 1 can compute one particular eigenpair approximation [59].

5 Numerical examples

In this section, we provide four numerical examples to validate the proposed augmented subspace algorithm and the corresponding theoretical analysis. Since the software FreeFEM++ offers a fast interpolation algorithm and a language to manipulate the data on multiple meshes, the methods in this paper is implemented with FreeFEM++ [28, 32]. With the help of finite element package FreeFem++ [28, 32], the numerical experiments are carried out on LSSC-IV in the State Key Laboratory of Scientific and Engineering Computing, Academy of Mathematics and Systems Science, Chinese Academy of Sciences. Each computing node has two 18-core Intel Xeon Gold 6140 processors at 2.3 GHz and 192 GB memory. The linear equation (3.1) in Algorithm 1 is solved by the package PETSc [4, 5, 6] with the aggregation-based AMG from Hypre (BoomerAMG) [19]. Each AMG step includes 5 V-cycle with Falgout coarsening scheme, one hybrid smoother from Symmetric Gauss Seidel and Jacobi iterations. The eigenvalue problem (3.3) is solved by the Krylov-Schur algorithm from Slep3 [43]. Here, the eigenpair approximation $(\bar{\lambda}_h, \bar{u}_h)$ of (2.7) is chosen as the exact one eigenpair to measure the errors of the approximations by the proposed algorithms.

5.1 Two dimensional examples

In the first subsection, we investigate the convergence and efficiency of Algorithms 1 and 2 for two dimensional eigenvalue problems.

Example 1

In the first example, we consider the elliptic eigenvalue problem with a piecewise constant coefficient and the computing domain has two circle interfaces. The nonnested augmented subspace method defined by Algorithm 1 is adopted to solve the following eigenvalue problem: Find (λ, u) such that

$$\begin{cases} -\nabla \cdot (\mathcal{K} \nabla u) &= \lambda u, & \text{in } \Omega, \\ [u] = 0, \quad [\mathbf{n}_\Gamma \mathcal{A} \nabla u] &= 0, & \text{on } \Gamma, \\ u &= 0, & \text{on } \partial\Omega. \end{cases} \quad (5.1)$$

Here, the computing domain $\Omega = (0, 2) \times (0, 2)$ includes two circles Ω_1 and Ω_2 with radius size 0.5 and centers $(2/3, 1)$ and $(4/3, 1)$, respectively. The coefficient \mathcal{K} in (5.1) is defined as follows

$$\mathcal{K} = \begin{cases} 10, & \text{in } \Omega_1 = \{(x, y) \in \mathbb{R}^2 | (x - 2/3)^2 + (y - 1)^2 \leq 1/9\}, \\ 10, & \text{in } \Omega_2 = \{(x, y) \in \mathbb{R}^2 | (x - 4/3)^2 + (y - 1)^2 \leq 1/9\}, \\ 1, & \text{in } \Omega_3 = \Omega / (\bar{\Omega}_1 \cup \bar{\Omega}_2). \end{cases} \quad (5.2)$$

In order to check the effect of the coarse mesh \mathcal{T}_H on the convergence rate, which is shown in Theorems 3.1 and 4.1, Corollary 3.1, we select two coarse meshes shown in Figure 2 for the test. For comparison, the finest mesh is chosen with the same 364416 elements for the two cases of coarse meshes.

Here, we check the numerical results for the first 4 eigenfunctions and 10 eigenvalues. Since the second and third exact eigenvalues are multiple, we need to do the following spectral projection for the eigenfunction approximations $u_{2,h}$ and $u_{3,h}$ as follows:

$$a(E_{2,3}w, v_h) = a(w, v_h), \quad \forall v_h \in \text{span}\{\bar{u}_{1,h}, \bar{u}_{2,h}\}.$$

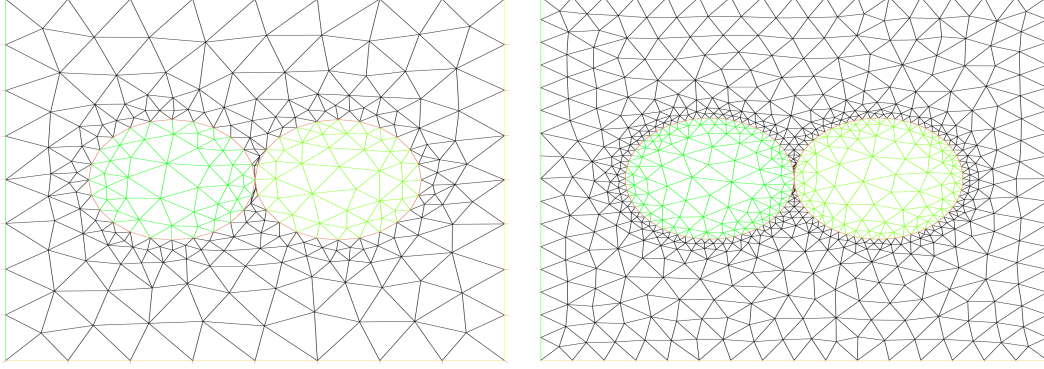


Figure 2: Two coarse meshes \mathcal{T}_H for Example 1: The left coarse mesh consists of 550 elements, and the right one 1456 elements.

Then the error estimate for the first 4 eigenfunction approximations can be defined as

$$\|u_{1,h} - \bar{u}_{1,h}\|_a + \|u_{2,h} - E_{2,3}u_{2,h}\|_a + \|u_{3,h} - E_{2,3}u_{3,h}\|_a + \|u_{4,h} - \bar{u}_{4,h}\|_a,$$

where $\bar{u}_{i,h}$ ($1 \leq i \leq 4$) denote the first 4 exact finite element eigenfunctions defined on the corresponding finer mesh \mathcal{T}_h .

When the coarse mesh is chosen as the left one in Figure 2, the corresponding numerical results are shown in Figure 3. Figure 4 presents the corresponding numerical results for the coarse mesh

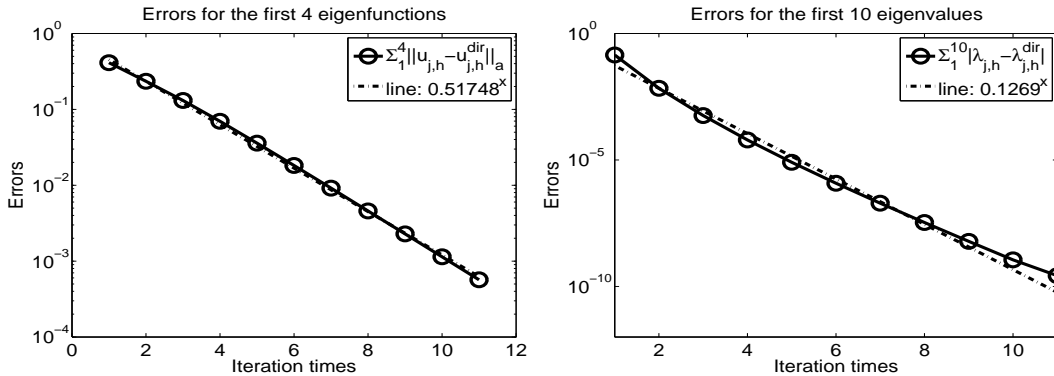


Figure 3: Error estimates for the first 4 eigenfunction and 10 eigenvalue approximations by Algorithm 2. Here the coarse mesh is chosen as the left one in Figure 2.

is chosen as the right one in Figure 2. From Figures 3 and 4, we can find that the finer mesh \mathcal{T}_H has faster convergence speed which validates theoretical results in Theorems 3.1 and 4.1, Corollary 3.1.

Furthermore, in order to check the efficiency of the proposed algorithms, we also investigate the CPU time for computing the first 10 eigenpair approximations. Here, the convergence criterion is set to be $|\lambda_h - \bar{\lambda}_h| < 1e-9$. Figure 5 shows the corresponding CPU time when the coarse meshes are chosen as the two in Figure 2. The results in Figure 5 validate the estimate of computational work in Theorem 4.2.

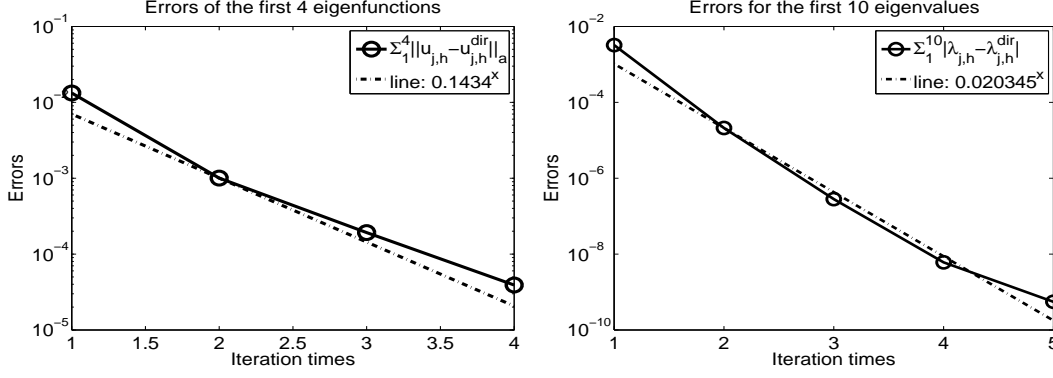


Figure 4: Error estimates for the first 4 eigenfunction and 10 eigenvalue approximations by Algorithm 2. Here the coarse mesh is chosen as the right one in Figure 2.

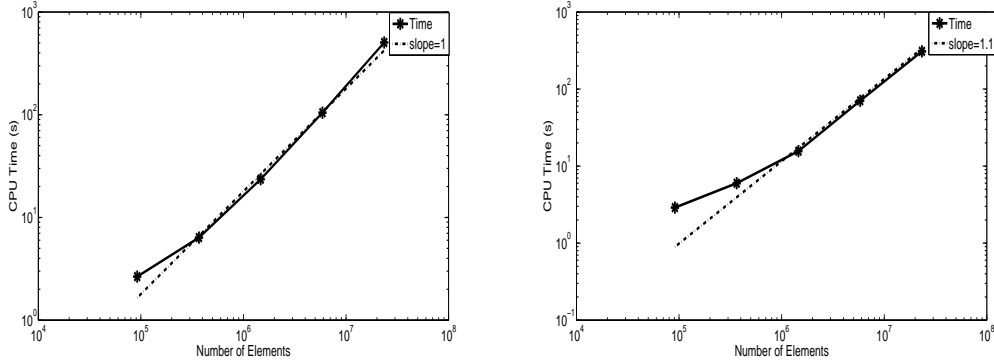


Figure 5: CPU time for Algorithm 2 with 32 processors, the left subfigure shows the CPU time when the coarse mesh is chosen as the left one in Figure 2 and the right subfigure shows the CPU time when the coarse mesh is chosen as the right one in Figure 2.

Example 2

In the second example, we also solve the eigenvalue problem (5.1). Here, the computing domain $\Omega = (0, 2) \times (0, 2)$ is partitioned into five parts by four circles with the radius 0.25 and centers $(0.5, 0.5)$, $(1.5, 0.5)$, $(0.5, 1.5)$ and $(1.5, 1.5)$, respectively. The coefficient \mathcal{K} in (5.1) is defined as follows

$$\mathcal{K} = \begin{cases} 10, & \text{in } \Omega_1 = \{(x, y) \in \mathbb{R}^2 | (x - 0.5)^2 + (y - 0.5)^2 \leq 1/16\}, \\ 10, & \text{in } \Omega_2 = \{(x, y) \in \mathbb{R}^2 | (x - 1.5)^2 + (y - 0.5)^2 \leq 1/16\}, \\ 10, & \text{in } \Omega_3 = \{(x, y) \in \mathbb{R}^2 | (x - 0.5)^2 + (y - 1.5)^2 \leq 1/16\}, \\ 10, & \text{in } \Omega_4 = \{(x, y) \in \mathbb{R}^2 | (x - 1.5)^2 + (y - 1.5)^2 \leq 1/16\}, \\ 1, & \text{in } \Omega_5 = \Omega / (\bar{\Omega}_1 \cup \bar{\Omega}_2 \cup \bar{\Omega}_3 \cup \bar{\Omega}_4). \end{cases}$$

In order to investigate the effect of the coarse mesh \mathcal{T}_H on the convergence rate of the nonnested augmented subspace method, we also choose two meshes shown in Figure 6 for the test. For the comparison, we select the same finest mesh which consists of 441600 elements for this example. In this example, we check the convergence behavior for computing the first 12 eigenfunction and 20 eigenvalue approximations.

When the left mesh of Figure 6 acts as the coarse mesh \mathcal{T}_H , Figure 7 presents the corresponding numerical results for the first 12 eigenfunction and 20 eigenvalue approximations. When the coarse

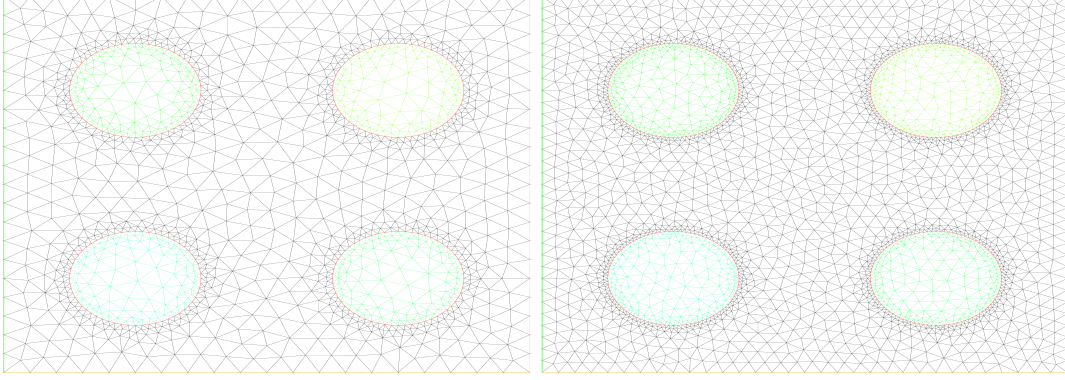


Figure 6: Two coarse meshes \mathcal{T}_H for Example 2: The left coarse mesh consists of 838 elements, and the right one 1992 elements.

mesh \mathcal{T}_H is chosen as the right one in Figure 6, the numerical results are shown in Figure 8. From

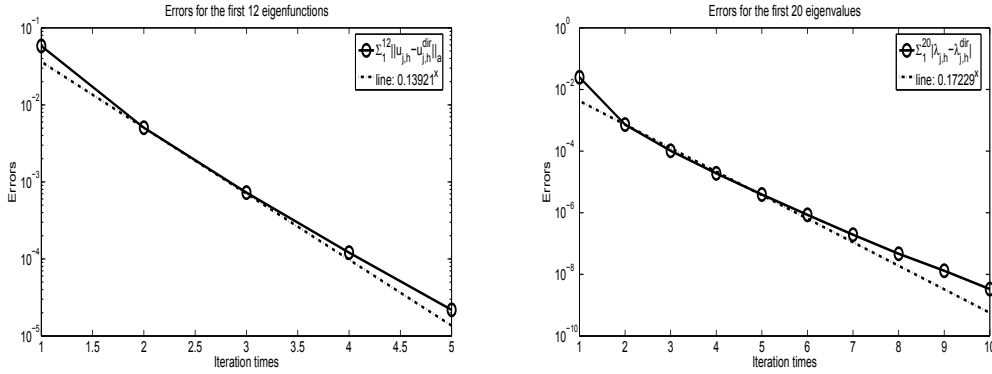


Figure 7: Error estimates for the first 12 eigenfunction and 20 eigenvalue approximations by Algorithm 2. Here the coarse mesh is chosen as the left one in Figure 6.

Figures 7 and 8, we can also find that finer mesh \mathcal{T}_H can lead to faster convergence speed which validates Theorem 3.1 and Corollary 3.1.

Similarly, we also investigate the efficiency with the CPU time for computing the first 10 eigen-pair approximations. Here the convergence criterion is set to be $|\lambda_h - \bar{\lambda}_h| < 1e-8$. Figure 9 shows the corresponding CPU time when the coarse meshes are chosen as the two in Figure 6 and the results also validate Theorem 4.2.

5.2 Three dimensional experiments

In the second subsection, the convergence and efficiency of Algorithms 1 and 2 are investigated for computing three dimensional eigenvalue problems.

Example 3

In this example, we consider the elliptic eigenvalue problem (5.1) with a piecewise constant coefficient on the three dimensional domain Ω which includes a spherical surface interface. The computing domain $\Omega = (0, 2) \times (0, 2) \times (0, 2)$ is divided into two parts by the surface of the sphere

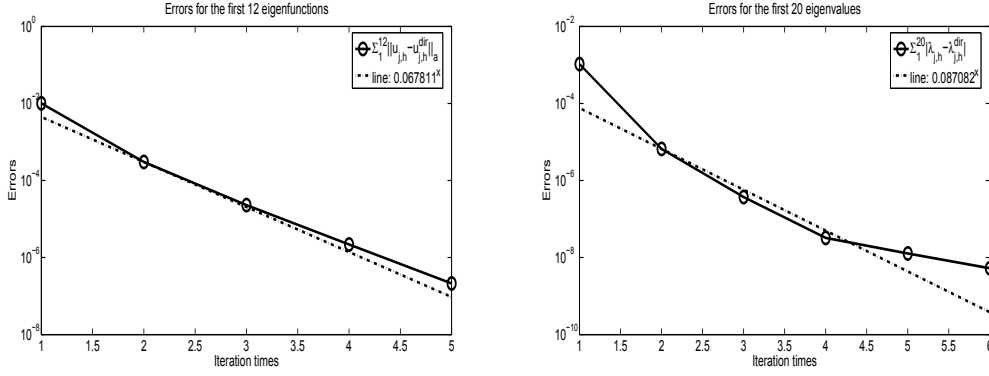


Figure 8: Error estimates for the first 12 eigenfunction and 20 eigenvalue approximations by Algorithm 2. Here the coarse mesh is chosen as the right one in Figure 6.

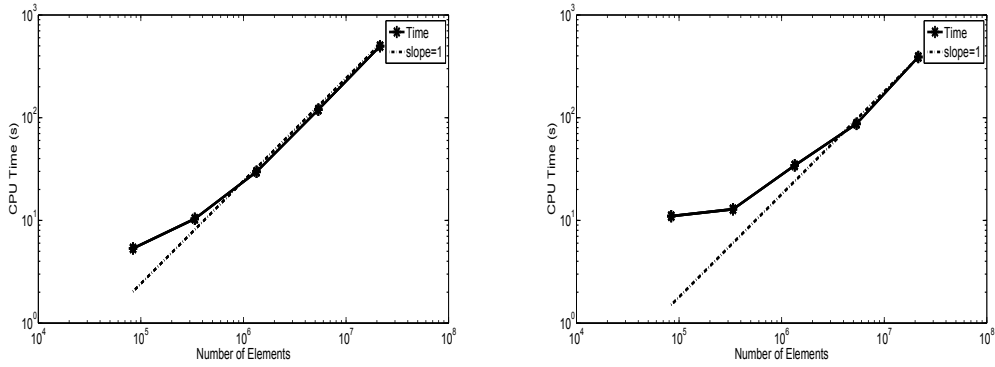


Figure 9: CPU time for Algorithm 2 with 32 processors, the left subfigure shows the CPU time when the coarse mesh is chosen as the left one in Figure 6 and the right subfigure shows the CPU time when the coarse mesh is chosen as the right one in Figure 6.

Ω_1 with center $(1, 1, 1)$ and radius 0.5. Here, the coefficient \mathcal{K} is defined as follows

$$\mathcal{K} = \begin{cases} 1, & \text{in } \Omega_1 = \{(x, y, z) \in \mathbb{R}^3 | (x-1)^2 + (y-1)^2 + (z-1)^2 \leq 1/4\}, \\ 10, & \text{in } \Omega_2 = \Omega / \Omega_1. \end{cases} \quad (5.3)$$

Similarly, in order to investigate the effect of the coarse grid \mathcal{T}_H on the convergence behavior, this example also selects two coarse meshes as shown in Figure 10. For comparison, we use the same finest mesh with 650145 elements for our test in this example. Here, we check the convergence for the first 4 eigenfunction and 10 eigenvalue approximations. When the coarse meshes \mathcal{T}_H are chosen as the left one and right one in Figure 10, the corresponding numerical results are shown in Figures 11 and 12, respectively. From Figures 11 and 12, we can find that the finer \mathcal{T}_H has better convergence rate, which validates the theoretical results in Theorem 3.1 and Corollary 3.1.

In order to check the efficiency of the proposed algorithms in this paper, we also check the CPU time for computing the first 10 eigenpair approximations. The convergence criterion is set to be $|\lambda_h - \bar{\lambda}_h| < 1e-9$. Figure 13 shows the CPU time results corresponding to the two coarse meshes in Figure 10. The results here also show the linear scale of the complexity for Algorithm 2 for the three dimensional eigenvalue problems with curved interfaces.

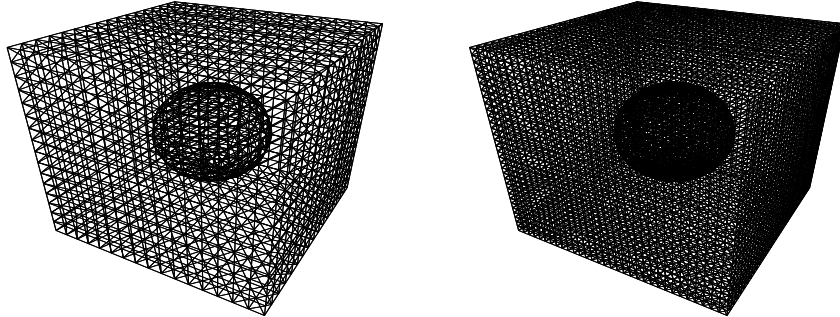


Figure 10: Two coarse meshes \mathcal{T}_H for Example 3: The left coarse mesh consists of 13169 elements, and the right one 40748 elements.

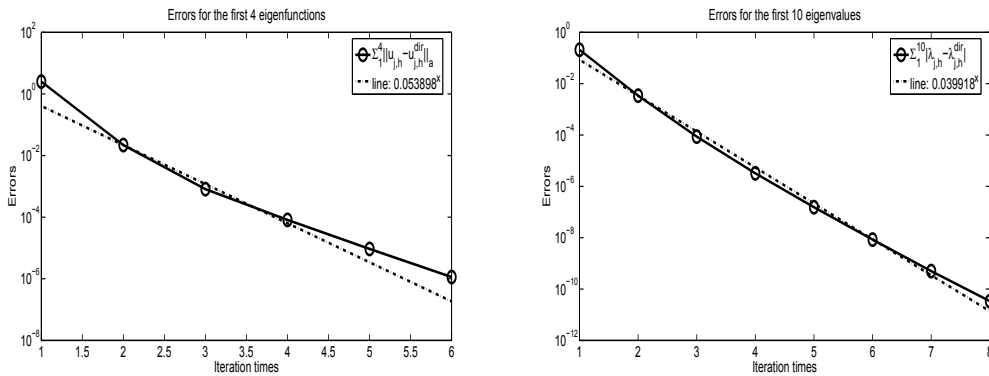


Figure 11: Error estimates for the first 4 eigenfunction and 10 eigenvalue approximations by Algorithm 2. Here the coarse mesh is chosen as the left one in Figure 10.

Example 4

In this example, we focus on the three-dimensional elliptic eigenvalue problem (5.1) with a piecewise constant coefficient which is defined on the three-dimensional domain $\Omega = (0, 2) \times (0, 2) \times (0, 2)$ with curve interfaces by two spheres. The computing domain is partitioned into three parts by two spheres with centers $(0.5, 0.5, 0.5)$ and $(1.5, 1.5, 1.5)$ and radius sizes 1.3 and $1/3$, respectively. The coefficient \mathcal{K} is defined as follows

$$\mathcal{K} = \begin{cases} 10, & \text{in } \Omega_1 = \{(x, y, z) \in \mathbb{R}^3 | (x - 0.5)^2 + (y - 0.5)^2 + (z - 0.5)^2 \leq 1/9\}, \\ 10, & \text{in } \Omega_2 = \{(x, y, z) \in \mathbb{R}^3 | (x - 1.5)^2 + (y - 1.5)^2 + (z - 1.5)^2 \leq 1/9\}, \\ 1, & \text{in } \Omega / (\bar{\Omega}_1 \cup \bar{\Omega}_2). \end{cases} \quad (5.4)$$

Here, we also select two coarse meshes as shown in Figure 14 for our tests. For comparison, we use the same finest mesh with 1178024 elements for checking the convergence behaviors.

Figure 15 and 16 show the numerical results for the first 4 eigenfunction and 11 eigenvalue approximations when the coarse meshes are chosen as the left and right ones in Figure 14. From

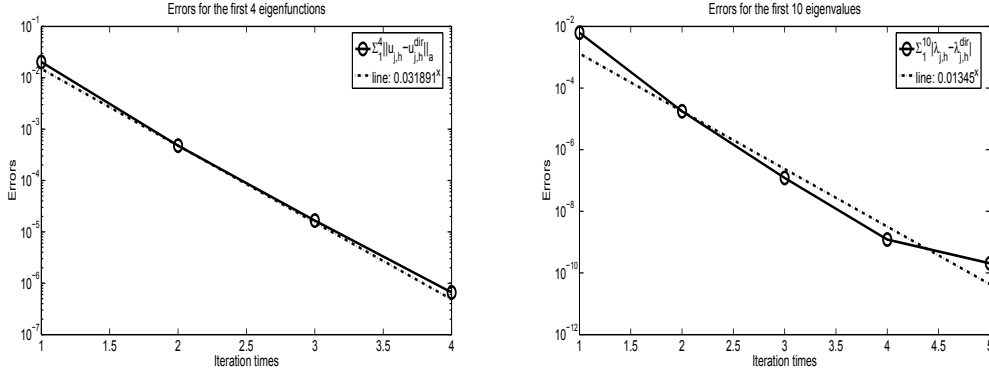


Figure 12: Error estimates for the first 4 eigenfunction and 10 eigenvalue approximations by Algorithm 2. Here the coarse mesh is chosen as the right one in Figure 10.

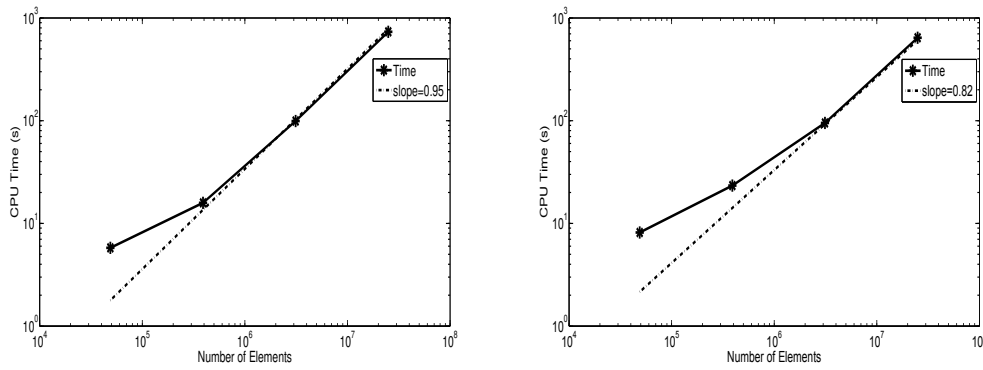


Figure 13: CPU time for Algorithm 2 with 16 processors, the left subfigure shows the CPU time when the coarse mesh is chosen as the left one in Figure 10 and the right subfigure shows the CPU time when the coarse mesh is chosen as the right one in Figure 10.

these two figures, we can also find the finer \mathcal{T}_H leads to faster convergence speed which confirm the theoretical results in Theorems 3.1 and 4.1, Corollary 3.1.

Here, we also present the CPU time results for computing the first 11 eigenpair approximations. The convergence criterion is also set to be $|\lambda_h - \bar{\lambda}_h| < 1e-9$. Figure 17 shows the CPU time results corresponding to the two coarse meshes in Figure 14. The results here also show the linear scale of the complexity for Algorithm 2 for the three dimensional eigenvalue problems with curved interfaces.

6 Conclusions

In this paper, we design a nonnested augmented subspace method and the corresponding multilevel correction scheme for solving eigenvalue problems with curved interfaces. Throughout this paper, we demonstrate that the augmented subspace method can also work on the nonnested sequence of meshes. The proposed algorithms here provide a way to combine the augmented subspace method (multilevel correction method) with the moving mesh techniques. This will improve the overall efficiency for solving the eigenvalue problems with anisotropy and singularity. The method in this paper can be extended to nonlinear eigenvalue problems and this will be our future work.

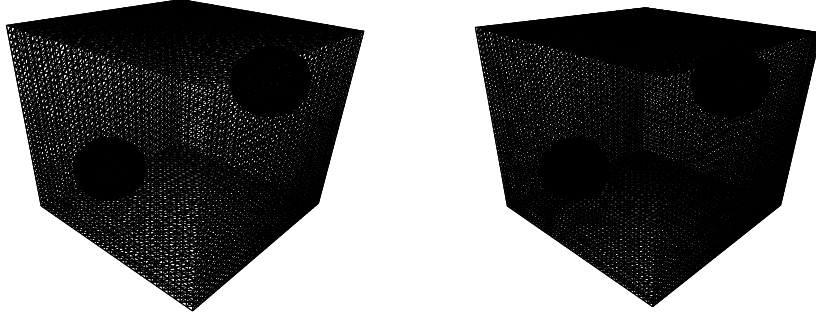


Figure 14: Two coarse meshes \mathcal{T}_H for Example 4: The left coarse mesh consists of 56660 elements, and the right one 92453 elements.

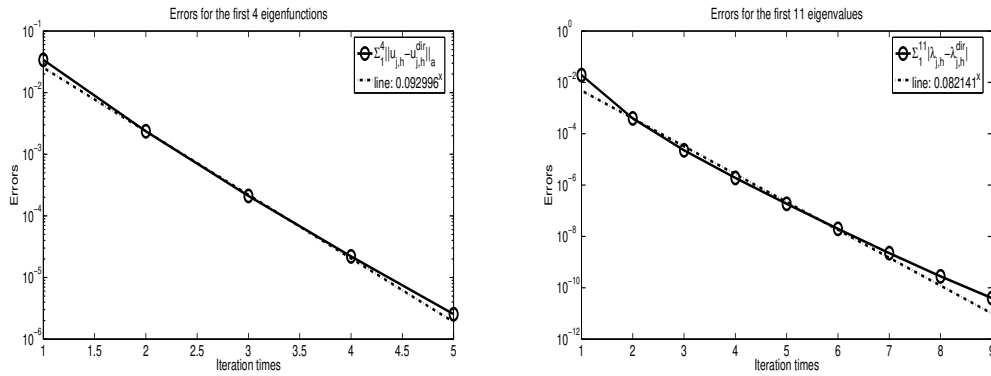


Figure 15: Error estimates for the first 4 eigenfunction and 11 eigenvalue approximations by Algorithm 2. Here the coarse mesh is chosen as the left one in Figure 14.

Acknowledgments

We are very grateful to Prof. Pierre Jolivet for his kind discussion and help to implement numerical examples with FreeFEM++. Especially, Prof. Pierre Jolivet help us to do the efficient interpolation between two nonnested meshes which is very important for implementing the proposed method in this paper. Here, we express our thanks for all developers of FreeFEM++.

References

- [1] R. A. Adams, *Sobolev Spaces*, Academic Press [A subsidiary of Harcourt Brace Jovanovich, Publishers], New York-London, 1975. Pure and Applied Mathematics, Vol. 65.

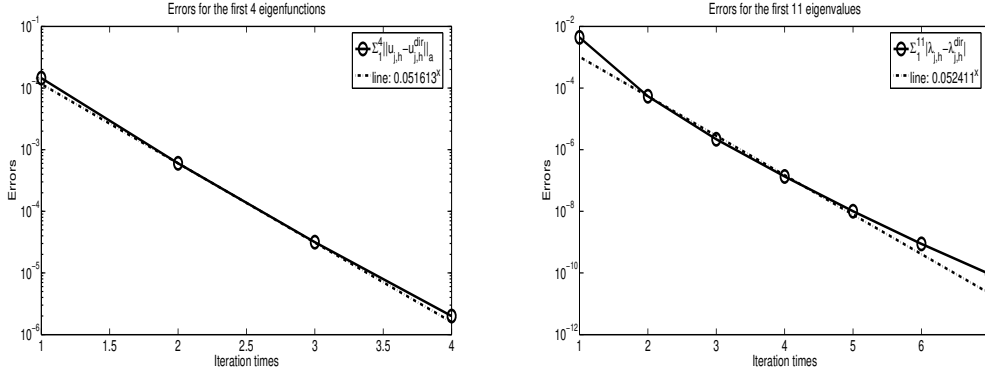


Figure 16: Error estimates for the first 4 eigenfunction and 11 eigenvalue approximations by Algorithm 2. Here the coarse mesh is chosen as the right one in Figure 14.

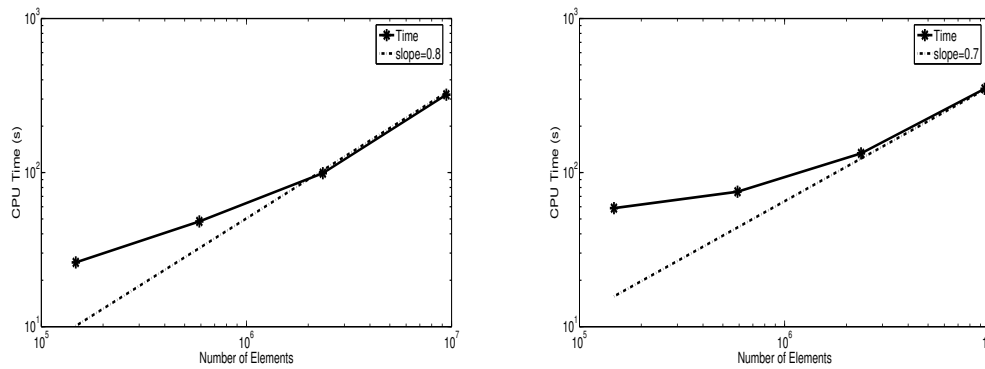


Figure 17: CPU time for Algorithm 2 with 16 processors, the left subfigure shows the CPU time when the coarse mesh is chosen as the left one in Figure 14 and the right subfigure shows the CPU time when the coarse mesh is chosen as the right one in Figure 14.

- [2] I. Babuška, *The finite element method for elliptic equations with discontinuous coefficients*, Computing, 5 (1970), pp. 207–213.
- [3] I. Babuška and J. E. Osborn, *Finite element-Galerkin approximation of the eigenvalues and eigenvectors of selfadjoint problems*, Math. Comp., 52 (1989), pp. 275–297.
- [4] S. Balay, S. Abhyankar, M. F. Adams, J. Brown, P. Brune, K. Buschelman, L. Dalcin, A. Dener, V. Eijkhout, W. D. Gropp, D. Karpeyev, D. Kaushik, M. G. Knepley, D. A. May, L. C. McInnes, R. T. Mills, T. Munson, K. Rupp, P. Sanan, B. F. Smith, S. Zampini, H. Zhang, and H. Zhang, *PETSc Web page*. <https://www.mcs.anl.gov/petsc>, 2019.
- [5] ———, *PETSc users manual*, Tech. Report ANL-95/11 - Revision 3.14, Argonne National Laboratory, 2020.
- [6] S. Balay, W. D. Gropp, L. C. McInnes, and B. F. Smith, *Efficient management of parallelism in object oriented numerical software libraries*, in Modern Software Tools in Scientific Computing, E. Arge, A. M. Bruaset, and H. P. Langtangen, eds., Birkhäuser Press, 1997, pp. 163–202.
- [7] R. E. Bank and T. Dupont, *An optimal order process for solving finite element equations*, Math. Comp., 36 (1981), pp. 35–51.

- [8] J. H. Bramble, *Multigrid Methods*, vol. 294 of Pitman Research Notes in Mathematics Series, Longman Scientific & Technical, Harlow; copublished in the United States with John Wiley & Sons, Inc., New York, 1993.
- [9] J. H. Bramble and J. E. Pasciak, *New convergence estimates for multigrid algorithms*, *Math. Comp.*, 49 (1987), pp. 311–329.
- [10] J. H. Bramble and X. Zhang, *The analysis of multigrid methods*, in *Handbook of Numerical Analysis*, Vol. VII, *Handb. Numer. Anal.*, VII, North-Holland, Amsterdam, 2000, pp. 173–415.
- [11] A. Brandt, S. McCormick, and J. Ruge, *Multigrid methods for differential eigenproblems*, *SIAM J. Sci. Statist. Comput.*, 4 (1983), pp. 244–260.
- [12] S. C. Brenner and L. R. Scott, *The Mathematical Theory of Finite Element Methods*, vol. 15 of *Texts in Applied Mathematics*, Springer-Verlag, New York, 1994.
- [13] F. Chatelin, *Spectral Approximation of Linear Operators*, *Computer Science and Applied Mathematics*, Academic Press, Inc. [Harcourt Brace Jovanovich, Publishers], New York, 1983. With a foreword by P. Henrici, With solutions to exercises by Mario Ahués.
- [14] H. Chen, Y. He, Y. Li, and H. Xie, *A multigrid method for eigenvalue problems based on shifted-inverse power technique*, *Eur. J. Math.*, 1 (2015), pp. 207–228.
- [15] H. Chen, H. Xie, and F. Xu, *A full multigrid method for eigenvalue problems*, *J. Comput. Phys.*, 322 (2016), pp. 747–759.
- [16] Z. Chen and J. Zou, *The finite element method for elliptic equations with discontinuous coefficients*, *Numerische Mathematik*, 79 (1998).
- [17] P. G. Ciarlet, *The Finite Element Method for Elliptic Problems*, vol. 4, North-Holland Publishing Co., Amsterdam-New York-Oxford, 1978. *Studies in Mathematics and its Applications*.
- [18] Y. Di, R. Li, T. Tang, and P. Zhang, *Moving mesh finite element method for the incompressible Navier-Stokes equations*, *SIAM J. Sci. Comput.*, 26 (2005).
- [19] R. D. Falgout and U. M. Yang, *hypre: A library of high performance preconditioners*, in *Computational Science — ICCS 2002*, P. M. A. Sloot, A. G. Hoekstra, C. J. K. Tan, and J. J. Dongarra, eds., Berlin, Heidelberg, 2002, Springer Berlin Heidelberg, pp. 632–641.
- [20] W. Gong, H. Xie, and N. Yan, *A multilevel correction method for optimal controls of elliptic equations*, *SIAM J. Sci. Comput.*, 37 (2015), pp. A2198–A2221.
- [21] ———, *Adaptive multilevel correction method for finite element approximations of elliptic optimal control problems*, *J. Sci. Comput.*, 72 (2017), pp. 820–841.
- [22] W. Hackbusch, *On the computation of approximate eigenvalues and eigenfunctions of elliptic operators by means of a multi-grid method*, *SIAM J. Numer. Anal.*, 16 (1979), pp. 201–215.
- [23] W. Hackbusch, *Multigrid methods and applications*, vol. 4 of *Springer Series in Computational Mathematics*, Springer-Verlag, Berlin, 1985.
- [24] J. Han, Y. Yang, and H. Bi, *A new multigrid finite element method for the transmission eigenvalue problems*, *Appl. Math. Comput.*, 292 (2017), pp. 96–106.
- [25] X. Han, Y. Li, and H. Xie, *A multilevel correction method for Steklov eigenvalue problem by nonconforming finite element methods*, *Numer. Math. Theory Methods Appl.*, 8 (2015), pp. 383–405.

- [26] X. Han, Y. Li, H. Xie, and C. You, *Local and parallel finite element algorithm based on multilevel discretization for eigenvalue problems*, Int. J. Numer. Anal. Model., 13 (2016), pp. 73–89.
- [27] X. Han, H. Xie, and F. Xu, *A cascadic multigrid method for eigenvalue problem*, J. Comput. Math., 35 (2017), pp. 74–90.
- [28] F. Hecht, *New development in freefem++*, Journal of Numerical Mathematics.
- [29] G. Hu, H. Xie, and F. Xu, *A multilevel correction adaptive finite element method for Kohn-Sham equation*, J. Comput. Phys., 355 (2018), pp. 436–449.
- [30] X. Ji, J. Sun, and H. Xie, *A multigrid method for Helmholtz transmission eigenvalue problems*, J. Sci. Comput., 60 (2014), pp. 276–294.
- [31] S. Jia, H. Xie, M. Xie, and F. Xu, *A full multigrid method for nonlinear eigenvalue problems*, Sci. China Math., 59 (2016), pp. 2037–2048.
- [32] P. Jolivet, F. Hecht, F. Nataf, and C. Prud’homme, *Scalable domain decomposition preconditioners for heterogeneous elliptic problems*, in SC ’13: Proceedings of the International Conference on High Performance Computing, Networking, Storage and Analysis, 2013, pp. 1–11.
- [33] J. Li, J. M. Melenk, B. Wohlmuth, and J. Zou, *Optimal a priori estimates for higher order finite elements for elliptic interface problems*, Applied Numerical Mathematics, 60 (2010), pp. 19–37.
- [34] R. Li, T. Tang, and P. Zhang, *Moving mesh methods in multiple dimensions based on harmonic maps*, J. Comput. Phys., 170 (2001), pp. 562–588.
- [35] ———, *A moving mesh finite element algorithm for singular problems in two and three space dimensions*, J. Comput. Phys., 177 (2002), pp. 365–393.
- [36] Q. Lin and H. Xie, *An observation on the Aubin-Nitsche lemma and its applications*, Math. Pract. Theory, 41 (2011), pp. 247–258.
- [37] ———, *A multilevel correction type of adaptive finite element method for Steklov eigenvalue problems*, in Applications of Mathematics 2012, Acad. Sci. Czech Repub. Inst. Math., Prague, 2012, pp. 134–143.
- [38] ———, *A multi-level correction scheme for eigenvalue problems*, Math. Comp., 84 (2015), pp. 71–88.
- [39] Q. Lin, H. Xie, and F. Xu, *Multilevel correction adaptive finite element method for semilinear elliptic equation*, Appl. Math., 60 (2015), pp. 527–550.
- [40] K. Miller, *Moving finite element methods II*, SIAM J. Numer. Anal., 18 (1981), pp. 1033–1057.
- [41] K. Miller and M. R. N., *Moving finite element methods I*, SIAM J. Numer. Anal., 18 (1981), pp. 1019–1032.
- [42] Z. Peng, H. Bi, H. Li, and Y. Yang, *A multilevel correction method for convection-diffusion eigenvalue problems*, Math. Probl. Eng., (2015), pp. Art. ID 904347, 10.
- [43] J. E. Roman, C. Campos, E. Romero, and A. Tomàs, *Slepc users manual—scalable library for eigenvalue problem computations*, Tech. Report 3.14, Universitat Politècnica de Valencia, Spain.

- [44] Y. Saad, *Numerical Methods for Large Eigenvalue Problems*, vol. 66 of Classics in Applied Mathematics, Society for Industrial and Applied Mathematics (SIAM), Philadelphia, PA, 2011. Revised edition of the 1992 original [1177405].
- [45] L. R. Scott and S. Zhang, *Higher-dimensional nonnested multigrid methods*, *Math. Comp.*, 58 (1992), pp. 457–466.
- [46] V. V. Shaidurov, *Multigrid Methods for Finite Elements*, vol. 318 of Mathematics and its Applications, Kluwer Academic Publishers Group, Dordrecht, 1995. Translated from the 1989 Russian original by N. B. Urusova and revised by the author.
- [47] A. Toselli and O. Widlund, *Domain Decomposition Methods—Algorithms and Theory*, vol. 34 of Springer Series in Computational Mathematics, Springer-Verlag, Berlin, 2005.
- [48] Y. Xi, X. Ji, and S. Zhang, *A multi-level mixed element scheme of the two-dimensional Helmholtz transmission eigenvalue problem*, *IMA J. Numer. Anal.*, 40 (2020), pp. 686–707.
- [49] H. Xie, *A multigrid method for eigenvalue problem*, *J. Comput. Phys.*, 274 (2014), pp. 550–561.
- [50] ———, *A type of multilevel method for the Steklov eigenvalue problem*, *IMA J. Numer. Anal.*, 34 (2014), pp. 592–608.
- [51] ———, *A multigrid method for nonlinear eigenvalue problems*, *Sci. Sin. Math.*, 45 (2015), pp. 1193–1204.
- [52] ———, *A type of multi-level correction scheme for eigenvalue problems by nonconforming finite element methods*, *BIT*, 55 (2015), pp. 1243–1266.
- [53] H. Xie and X. Wu, *A multilevel correction method for interior transmission eigenvalue problem*, *J. Sci. Comput.*, 72 (2017), pp. 586–604.
- [54] H. Xie and M. Xie, *A multigrid method for ground state solution of Bose-Einstein condensates*, *Commun. Comput. Phys.*, 19 (2016), pp. 648–662.
- [55] H. Xie, M. Xie, and N. Zhang, *An efficient multigrid method for semilinear elliptic equation*, *J. Num. Method. Comp. Appl.*, 40 (2019), pp. 143–160.
- [56] H. Xie, L. Zhang, and H. Owhadi, *Fast eigenpairs computation with operator adapted wavelets and hierarchical subspace correction*, *SIAM J. Numer. Anal.*, 57 (2019), pp. 2519–2550.
- [57] H. Xie and T. Zhou, *A multilevel finite element method for Fredholm integral eigenvalue problems*, *J. Comput. Phys.*, 303 (2015), pp. 173–184.
- [58] F. Xu and H. Xie, *A full multigrid method for semilinear elliptic equation*, *Appl. Math.*, 62 (2017), pp. 225–241.
- [59] F. Xu, H. Xie, and N. Zhang, *An eigenwise parallel augmented subspace method for eigenvalue problems*, arXiv: 1908.10251, (2019).
- [60] J. Xu, *Iterative methods by space decomposition and subspace correction*, *SIAM Rev.*, 34 (1992), pp. 581–613.
- [61] ———, *A new class of iterative methods for nonselfadjoint or indefinite problems*, *SIAM J. Numer. Anal.*, 29 (1992), pp. 303–319.
- [62] X. Xu, *Parallel algebraic multigrid methods: state-of-the art and challenges for extreme-scale applications*, *J. Num. Method. Comp. Appl.*, 40 (2019), pp. 243–260.

- [63] M. Yue, H. Xie, and M. Xie, *A cascadic multigrid method for nonsymmetric eigenvalue problem*, Appl. Numer. Math., 146 (2019), pp. 55–72.
- [64] N. Zhang, X. Han, Y. He, H. Xie, and C. You, *An algebraic multigrid method for eigenvalue problems in some different cases*, arXiv: 1503.08462, (2015).
- [65] N. Zhang, F. Xu, and H. Xie, *An efficient multigrid method for ground state solution of Bose-Einstein condensates*, Int. J. Numer. Anal. Model., 16 (2019), pp. 789–803.
- [66] S. Zhang, Y. Xi, and X. Ji, *A multi-level mixed element method for the eigenvalue problem of biharmonic equation*, J. Sci. Comput., 75 (2018), pp. 1415–1444.